Engineering Structures 86 (2015) 122–133

Contents lists available at ScienceDirect

Engineering Structures

journal homepage: www.elsevier.com/locate/engstruct

A three-phase, multi-component ionic transport model for simulation of chloride penetration in concrete

Qing-feng Liu [a,b,*], Dave Easterbrook [c], Jian Yang [a,b,d], Long-yuan Li [c]

[a] State Key Laboratory of Ocean Engineering, Shanghai Jiao Tong University, Shanghai 200240, PR China
[b] School of Naval Architecture, Ocean & Civil Engineering, Shanghai Jiao Tong University, Shanghai 200240, PR China
[c] School of Marine Science and Engineering, University of Plymouth, PL4 8AA, UK
[d] School of Civil Engineering, University of Birmingham, B15 2TT, UK

ARTICLE INFO

Article history:
Received 14 August 2014
Revised 27 December 2014
Accepted 29 December 2014

Keywords:
Chloride
Migration
Concrete
Aggregates
ITZ
Multi-phase
Multi-species
Ionic interaction
Binding

ABSTRACT

Chloride-induced corrosion of reinforcing steel in concrete is a serious problem in the durability of structures. In order to predict how chlorides penetrate in concrete, unlike most existing models which consider the penetration of only a single species or in a single phase medium, this paper presents a numerical model considering the transport of multiple species in a multi-phase medium. The 2-D, 3-phase, multi-component ionic transport model proposed in the paper also considers ionic binding and the model is used to simulate the rapid chloride migration (RCM) test of concrete. The effects of aggregates, ITZs and ionic binding on chloride penetration in concrete are examined and discussed. The obtained result is also validated against experimental data obtained in an accelerated chloride migration test.

© 2015 Elsevier Ltd. All rights reserved.

1. Introduction

Chloride-induced corrosion of reinforcing steel in concrete is a worldwide problem. It affects a large number of reinforced concrete structures, particularly those used in offshore or exposed in marine environment. In order to prevent reinforcing steel from corrosion one has to control the penetration of chlorides in concrete. By doing so, one has to know the mechanism about how chlorides penetrate in concrete and how individual components in concrete respond while chlorides enter the concrete.

Concrete is a composite material composed of aggregates embedded in a hard matrix of the cement paste that fills the space among the aggregates and glues them together. The cement particles in fresh concrete, which are suspended in the mix water, cannot pack together as efficiently when they are in the close vicinity of a much larger solid object, such an aggregate particle. This is due to the effect of shear stresses exerted on the cement paste by the aggregate particles during mixing, which tend to cause the water to separate from the cement particles. This results in a narrow region around the aggregate particles with fewer cement particles, and thus more water. This narrow region is usually called the interfacial transition zone (ITZ) [1–3].

ITZ has a higher water-to-cement ratio and thus a larger porosity, than the bulk cement paste. Images of SEM have shown that ITZ is not uniform, but varies with the distance from the aggregate particle [4,5]. The average thickness of ITZs found in a normal concrete is 20–40 μm, although it tends to be larger around larger aggregate particles. The ITZ has important effects on the mechanical properties and durability of concrete, because it tends to act as the "weak link in the chain" when compared with the bulk cement paste and the aggregate particles.

Extensive research has been carried out since early of 1980s to investigate how chlorides penetrate in concrete. The work involves the use of analytical, experimental, and numerical methods. The corresponding transport models so far developed can be categorised into four groups, as illustrated in Fig. 1. The first group is the transport model considering the penetration of a single species (i.e. chloride ions) in a single phase medium (i.e. idealised dilute solution) [6–11]. The second group is the transport model considering the transport of multiple species (such as chloride, hydroxyl,

* Corresponding author at: School of Naval Architecture, Ocean & Civil Engineering, Shanghai Jiao Tong University, Shanghai 200240, PR China. Tel.: +86 1394 2035 131.
E-mail addresses: henrylqf@163.com, liuqf@sjtu.edu.cn (Q.-f. Liu).

http://dx.doi.org/10.1016/j.engstruct.2014.12.043
0141-0296/© 2015 Elsevier Ltd. All rights reserved.

sodium and potassium ions) also in a single phase medium [12–21]. The third group is the transport model considering the penetration of a single species in a medium of multiple phases with different transport properties [22–37]. The forth group is the transport model considering the transport of multiple species also in a medium of multiple phases [38]. The models used in the third and fourth groups are also called the multi-phase model.

The main purpose of developing multi-phase transport models is to numerically investigate the effect of individual components of concrete such as aggregates and ITZs on the transport of chlorides, which cannot be fulfilled by using the 1-D model. For example, Zeng developed a 2-D, 2-phase FEA model to simulate the chloride diffusion in a heterogeneous concrete composed of aggregates and cement paste matrix, which have distinct chloride diffusivities [39]. His result showed that the chloride diffusion in the heterogeneous concrete lags behind the equivalent homogeneous concrete chloride diffusion predicted using an effective diffusion coefficient. Zheng and Zhou proposed a 3-phase spherical model to represent the heterogeneous nature of concrete and derived an analytical expression for chloride diffusion in concrete [40]. Later, Zheng et al. further investigated the influence of ITZs on the steady-state chloride diffusion in mortar and concrete materials using numerical simulations [41]. Recently, Zheng et al. developed a 2-D, 3-phase lattice model and investigated the shape effect of aggregates on chloride diffusion in concrete [42]. Li et al. developed 2-phase FEA models in both 2-D and 3-D to predict the effect of aggregates on the effective diffusion coefficient of chlorides [43]. Their result showed that the 2-D model produced a lower chloride diffusivity of concrete than the 3-D model does. The former is close to the lower bound of the effective diffusion coefficient of chlorides in concrete, whereas the latter agrees with that predicted by using Maxwell's equation. More recently, Abyaneh et al. developed a 3-D, 3-phase FEA model to investigate the effects of aggregates including the aspect-ratio and orientation of ellipse shape aggregates and ITZs on the diffusion coefficient of chlorides in concrete [44]. The effect of electrical double layer on ionic transport in cement-based materials was also investigated recently [45,46].

Note that most multi-phase numerical models mentioned above [39–44] also consider the penetration of only chloride ions. The interaction between different ionic species is not taken into account in these models. Existing studies have shown that ionic interactions have an important effect on the transport of chlorides in concrete, particularly when there is an external electric field involved [17–21]. Typical examples for such cases include the rapid chloride migration (RCM) tests and electrochemical chloride removal. In the previous 2-D, 2-phase FEA model [38] we considered the interaction between different ionic species and examined the effect of aggregates on the transport of various ionic species in concrete. However the model did not include ITZs and ionic binding. In this paper the previous 2-D, 2-phase FEA model [38] is further expanded to include ITZs and to take into account the ionic binding. The present 2-D, 3-phase, multi-component ionic transport model is used to simulate the RCM test of concrete, from which the effects of aggregates, ITZs and ionic binding on chloride penetration in concrete are discussed.

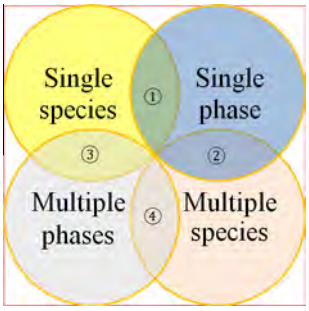

Fig. 1. Categories of ionic transport models in concrete. (1) Single phase and single species transport model, (2) single phase and multi-species transport model, (3) multi-phase and single species transport model, and (4) multi-phase and multi-species transport model.

Ideally, the multi-phase modelling of ionic transport in concrete should use a 3D geometric model, for example [44,47,48]. However, at present the 3D model can be applied only to the problems where the model has a single ionic species [44,47] or multiple ionic species but they are controlled by the electro-neutrality condition [48,49]. The reason for this is because in either case the migration speed is independent of ionic concentration, for which case the governing equations are linear and their solution can be achieved without numerical difficulty. However, the use of electro-neutrality condition leads to a decoupling of ionic transport between different ionic species, which is principally incorrect [20,50]. Therefore, one should use the Poisson equation, instead of the electro-neutrality condition [20,21,38]. The use of Poisson equation in the ionic transport model makes the transport equations not only highly nonlinear but also the coupling between different ionic species. As a consequence of this, the migration speed of individual ionic species may vary greatly with time and position. This makes very difficult to achieve convergent solutions unless the element sizes in the finite element mesh are extremely small [38,47]. This problem even gets worse when the ITZs are involved in the model. This is why most multiphase models, available today, use the 2-D rather than 3-D geometry. Note that although the variation of tortuosity with volume fraction in a 2-D geometry is not exactly the same as that in a 3-D geometry, the difference is not very significant [47,50]. Thus, the 2-D simulation can provide a good approximation, while the 3-D simulation results are not available.

2. Ionic transport in multi-component electrolyte solutions

The pore solution in concrete involves many ionic species including hydroxyl, sulphate, sodium, potassium, calcium, etc., among which the hydroxyl has the highest concentration, followed by the potassium and sodium. The transport of ions in a saturated concrete is mainly by two driving forces, known as the diffusion and migration. The former is due to the concentration gradient of the species itself; the latter is due to the electrostatic potential generated by an externally applied electric field and/or the internal charge imbalance between different species in the solution. In the presence of external electric field, positively charged ions will move towards cathode, whereas negatively charged ions will move towards anode. The opposite-direction movement between cations and anions will generate significant internal charge imbalance between cations and anions within the solution. This charge imbalance creates an electrostatic potential which can affect the transport of all ionic species in the solution. In the absence of external electric field, different ionic species having different diffusion coefficients travel in different speeds. This also generates charge imbalance between species and creates an electrostatic potential, which affects the transport of all ionic species in the solution. The exact effect of charge imbalance on the transport of ions in concrete is dependent on the external electric field applied and the difference of diffusion coefficients between ionic species. In general, the effect of charge imbalance on the ionic transport increases with the external electric field and the difference of diffusion coefficients between ionic species. Mathematically, the flux of an ionic species in a multi-component electrolyte solution can be expressed in terms of Nernst–Planck equation as follows,

$$\mathbf{J}_k = -D_k \nabla C_k - D_k C_k \frac{z_k F}{RT} \nabla \Phi \tag{1}$$

where $\mathbf{J}_k$ is the flux, C_k is the concentration, D_k is the diffusion coefficient, z_k is the charge number, $F = 9.648 \times 10^{-4}$ C mol^{-1} is the Faraday constant, $R = 8.314$ J mol^{-1} K^{-1} is the ideal gas constant, $T = 298$ K is the absolute temperature, Φ is the electrostatic potential, and the subscript k represents the kth ionic species. Eq. (2) is required for each ionic species involved in the solution owing to the mass conservation in unit volume of electrolyte solution,

$$\frac{\partial C_k}{\partial t} = -\nabla \cdot \mathbf{J}_k \tag{2}$$

where t is the time. Substituting Eqs. (1) and (2), it yields,

$$\frac{\partial C_k}{\partial t} = \nabla(D_k \nabla C_k) + \nabla\left[\left(\frac{z_k D_k F}{RT}\right) C_k \nabla \Phi\right] \tag{3}$$

Note that if the electrostatic potential, Φ, in Eq. (3) is purely determined in terms of the externally applied electric field without taking into account the internal charge imbalance between ionic species, that is $\nabla^2 \Phi = 0$, then the concentration of each ionic species can be calculated independently by using Eq. (3). Otherwise, the electrostatic potential has to be determined using Poisson's equation as follows,

$$\nabla^2 \Phi = -\frac{F}{\varepsilon_0 \varepsilon_r} \sum_{k=1}^{N} z_k C_k \tag{4}$$

where $\varepsilon_o = 8.854 \times 10^{-12}$ C V^{-1} m^{-1} is the permittivity of a vacuum, $\varepsilon_r = 78.3$ is the relative permittivity of water at temperature of 298 K, and N is the total number of species involved in the solution. The use of Poisson's equation creates two difficulties. One is the coupling of Eq. (3) between different ionic species, since Φ is now dependent on not only the boundary conditions governed by the externally applied electric field, but also the concentrations of all ionic species involved in the solution. The other is the nonlinearity and numerical difficulty which involves calculations of large and small numbers that need be handled carefully [38]. Nevertheless, Eqs. (3) and (4) plus initial and boundary conditions can be used to determine the electrostatic potential, Φ, and the concentrations of individual ionic species, C_k ($k = 1,2,\ldots,N$), at any point and any time in the solution domain.

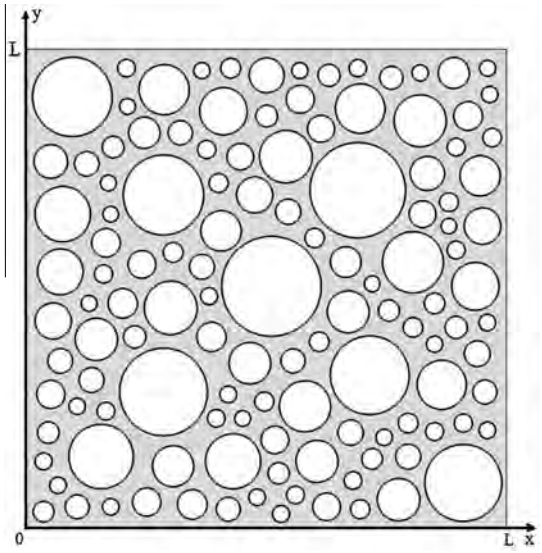

Fig. 2. The geometry of 3-phase mesoscale concrete model ($V_a = 0.5$, 100 μm thick ITZ).

3. Ionic transport in the medium of multi-phases

As aforementioned, concrete can be treated as a composite with aggregate-, cement paste- and ITZ-phases. Compared with the cement paste and ITZs, aggregates are much dense and have much high resistance to the transport of ions and therefore, in the present study they are assumed to be the impermeable material. The cement paste- and ITZ-phases can be treated as two individual porous materials with different transport properties. When applying the ionic transport equations from an electrolyte solution to a porous material, one has to consider the effects of porosity and tortuosity of the pore structure as well as the adsorption/desorption of ions at pore surfaces on the ionic transport in the porous material. The former is usually to be incorporated into the diffusion coefficient and the latter is often represented using ionic binding models. In this case, Eq. (2) need be modified as follows,

$$\frac{\partial(\varphi C_k)}{\partial t} + \frac{\partial[(1-\varphi)S_k]}{\partial t} = -\varphi \nabla \cdot \mathbf{J}_k \tag{5}$$

where φ is the porosity of the porous material and S_k is the concentration of bound ions. To eliminate φ and S_k in Eq. (5), the following Langmuir isotherm is often used to link the concentrations of bound and free ions,

$$\frac{(1-\varphi)S_k}{\varphi} = \frac{\alpha_k C_k}{w(1+\beta_k C_k)} \tag{6}$$

where w is the content of the water in which ionic transport takes place, expressed per unit weight of cement, α_k and β_k are the constants which can be determined experimentally. Note that other chloride binding isotherms such as the linear and Freundlish isotherms could also be used, which will result in Eq. (6) to have different expressions. For chloride ions the experimental results for the cement paste of $w = 0.3$ showed $\alpha_k = 0.42$ and $\beta_k = 0.8$ mol^{-1} l [8]. The use of Eqs. (1) and (6) in Eq. (5), yields,

$$(1+\lambda_k)\frac{\partial C_k}{\partial t} = \nabla(D_k \nabla C_k) + \nabla\left[\left(\frac{z_k D_k F}{RT}\right) C_k \nabla \Phi\right] \tag{7}$$

where $\lambda_k > 0$ is a dimensionless parameter for the kth species defined as follows,

$$\lambda_k = \frac{\alpha_k}{w(1+\beta_k C_k)^2} \tag{8}$$

Two features are revealed in Eq. (7). The first one is the ionic binding. It can be seen from Eq. (7) that the ionic binding will decrease the transport speed of ions. The second one is the form of the transport equation. In the absence of ionic binding, the transport equation of ions in a porous material is exactly the same as that in an electrolyte solution except that their diffusion coefficients are defined differently. In the former the diffusion coefficient is defined in the idealised dilute solution; whereas in the latter it is defined in the pore solution of the porous material. The value in the latter case is much smaller than that in the former case. A detailed discussion on the diffusion coefficient of ions in porous materials can be found in [51,52]. Eqs. (7) and (4) can be used to determine the electrostatic potential, Φ, and the concentrations of individual ionic species, C_k ($k = 1,2,\ldots,N$), at any point and any time in the domain of the porous material. Note that when Eqs. (4) and (7) are applied to the concrete material of aggregates, ITZs, and cement paste phases, one has to use different transport properties for aggregates, ITZs, and cement paste, whereas continuous conditions are imposed for ionic concentrations and ionic fluxes at the interfaces between different phases. The details of the geometric modelling of the concrete of multi-phases will be given in following section.

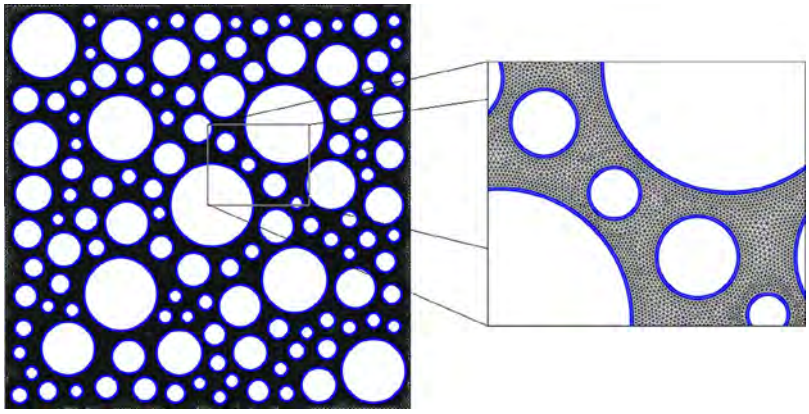

Fig. 3. Finite element mesh of the 3-phase concrete model (V_a = 0.5, 100 μm thick ITZ).

Table 1
Ionic transport properties in different phases.

Field variables	Potassium (mol/m^3)	Sodium (mol/m^3)	Chloride (mol/m^3)	Hydroxide (mol/m^3)
Charge number	1	1	−1	−1
Diffusion coefficient in aggregates	0	0	0	0
Diffusion coefficient in cement paste $\times 10^{-10}$ m^2/s	1.957	1.334	2.032	5.260
Diffusion coefficient in ITZs $\times 10^{-10}$ m^2/s	5.87	4.00	6.10	15.78

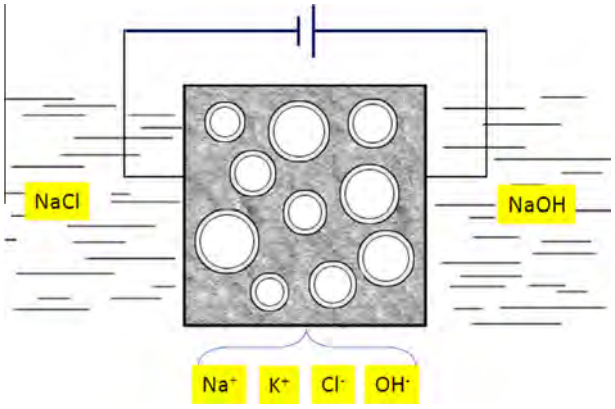

Fig. 4. Schematic representation of 2-D, 3-phase plain concrete specimen in a RCM test.

Also, it should be noted that the model described above does not take into account the activity coefficients of ionic species and the effect of electrical double layer on ionic transport. The effect of the former can be done by modifying diffusion coefficients, whereas that of the latter can be generally ignored in this study because the electrical double layer in concrete is highly compressed.

4. Finite element analysis model

To investigate the effects of aggregates, ITZs and ionic binding on the transport of ions in concrete, a series of 2-D, 3-phase FEA models with various different aggregate volume fractions are developed, in which the specimen is modelled as a square plate of a size of 50 mm × 50 mm. The aggregates are represented by a number of solid circles of radii ranging from 1.5 mm to 10 mm. These solid circles are randomly generated in the geometric model using MATLAB software. For each aggregate there is an ITZ surrounding it. Note that the concrete modelled here is assumed to be fully saturated due to the standard of RCM test [53–56] and therefore there are no air voids in the geometric model. Also, note that the real thickness of ITZs in normal concrete is only 20–40 μm. However, this kind of thin layer creates some difficulty in the element mesh of ITZs due to the limitation of element number used in computation. To avoid this problem the ITZ layer in the present model is artificially increased to 100 μm. However, in order not to overlook the effect of ITZs on the results, the increase of the ITZs volume in the model is compensated by the reduction of the diffusion coefficients of ions in the ITZs. Fig. 2 graphically displays one of the geometric models analysed, which involves solid circles, representing the impermeable aggregates, annual thin layers surrounding the solid circles, representing the ITZs, and the remaining space, representing the cement paste. Fig. 3 shows the

Table 2
Initial and boundary conditions of individual species.

Field variables	Potassium	Sodium	Chloride	Hydroxide	Electrostatic potential
Concentration boundary conditions					
$x = 0$	0	520 (mol/m^3)	520 (mol/m^3)	0	0
$x = L$	0	300 (mol/m^3)	0	300 (mol/m^3)	24 V
Flux boundary conditions					
$y = 0$	$J = 0$	$J = 0$	$J = 0$	$J = 0$	$\partial\Phi/\partial y = 0$
$y = L$	$J = 0$	$J = 0$	$J = 0$	$J = 0$	$\partial\Phi/\partial y = 0$
Initial conditions					
$t = 0$	200 (mol/m^3)	100 (mol/m^3)	0	300 (mol/m^3)	0

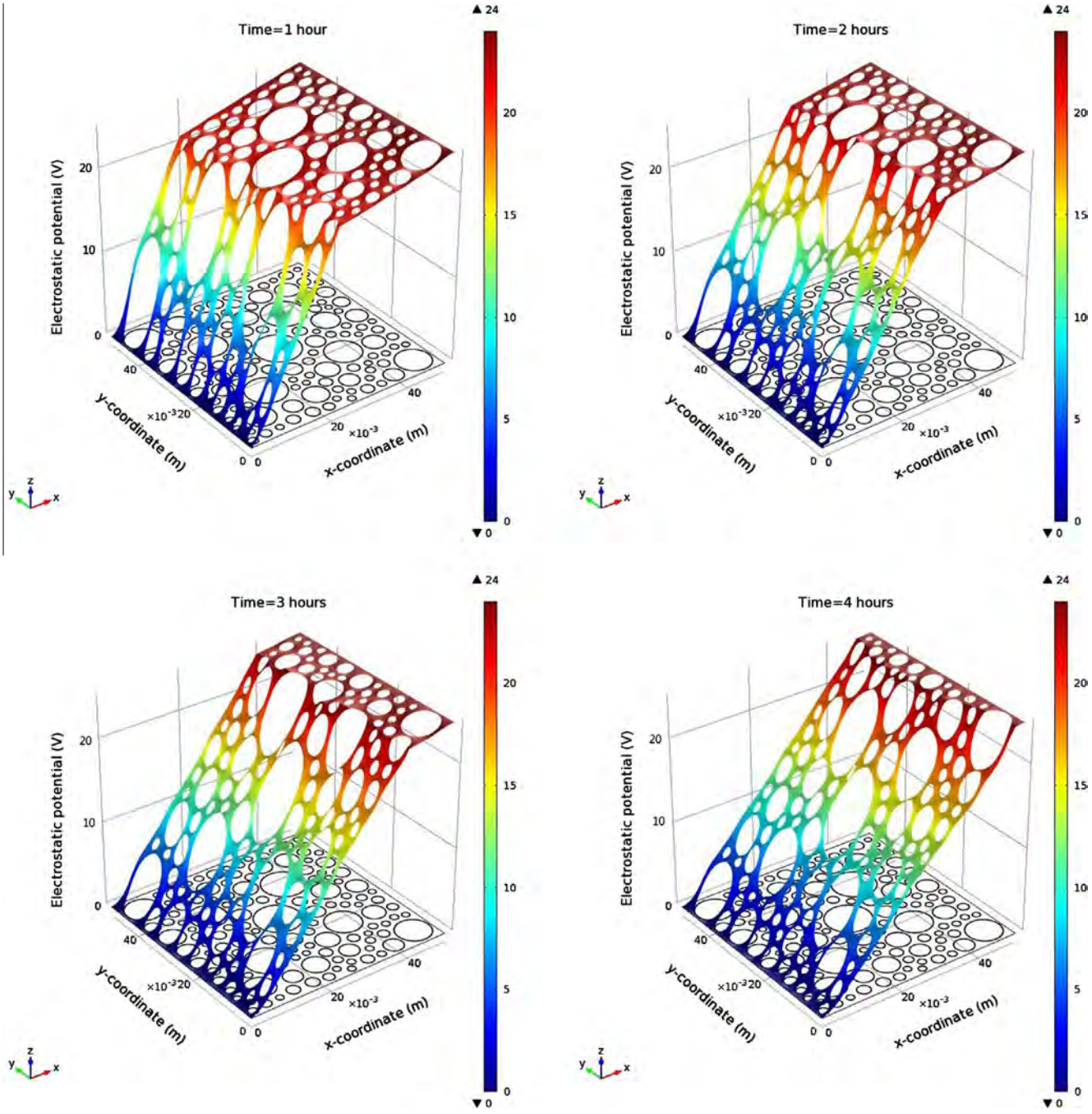

Fig. 5a. Electrostatic potential distribution profiles at four different times.

corresponding finite element mesh used. As the aggregates (white area) are assumed to be impermeable, they are not meshed in the models, which means that the ionic transport takes place only in the cement paste and ITZ phases although the diffusion coefficients are different in these two phases. The continuous conditions are assumed for both concentration and flux at the interface between the cement paste and ITZ phases.

Existing data showed that the ratio of diffusion coefficients between ITZs and bulk cement paste is about 4–15, depending on the porosity and water-to-cement ratio of individual specimens [34,40,52]. Considering the use of large thickness of ITZs in the geometric models, the diffusion coefficient in ITZ phase for each ionic species employed in the present study is taken as three times of that in cement paste phase. Table 1 shows the transport properties employed in the present study for aggregates, cement paste and ITZs. Note that the diffusion coefficients employed in the present multi-phase model is one-order higher than those normally used for cement materials but one-order lower than those provided for the dilute solution. This is because the effects of ionic binding and tortuosity on ionic transport are taken into account by the model itself not by the diffusion coefficients.

The 2-D, 3-phase concrete models are used to simulate the RCM test of concrete, in which the 50 mm × 50 mm plain concrete specimen is located between two compartments, one of which has a 0.52 mol/l NaCl solution, the other of which has a 0.30 mol/l NaOH solution. An external potential difference of 24 V is applied between two electrodes inserted into the two compartment solutions. The ionic species to be analysed in the simulations include potassium,

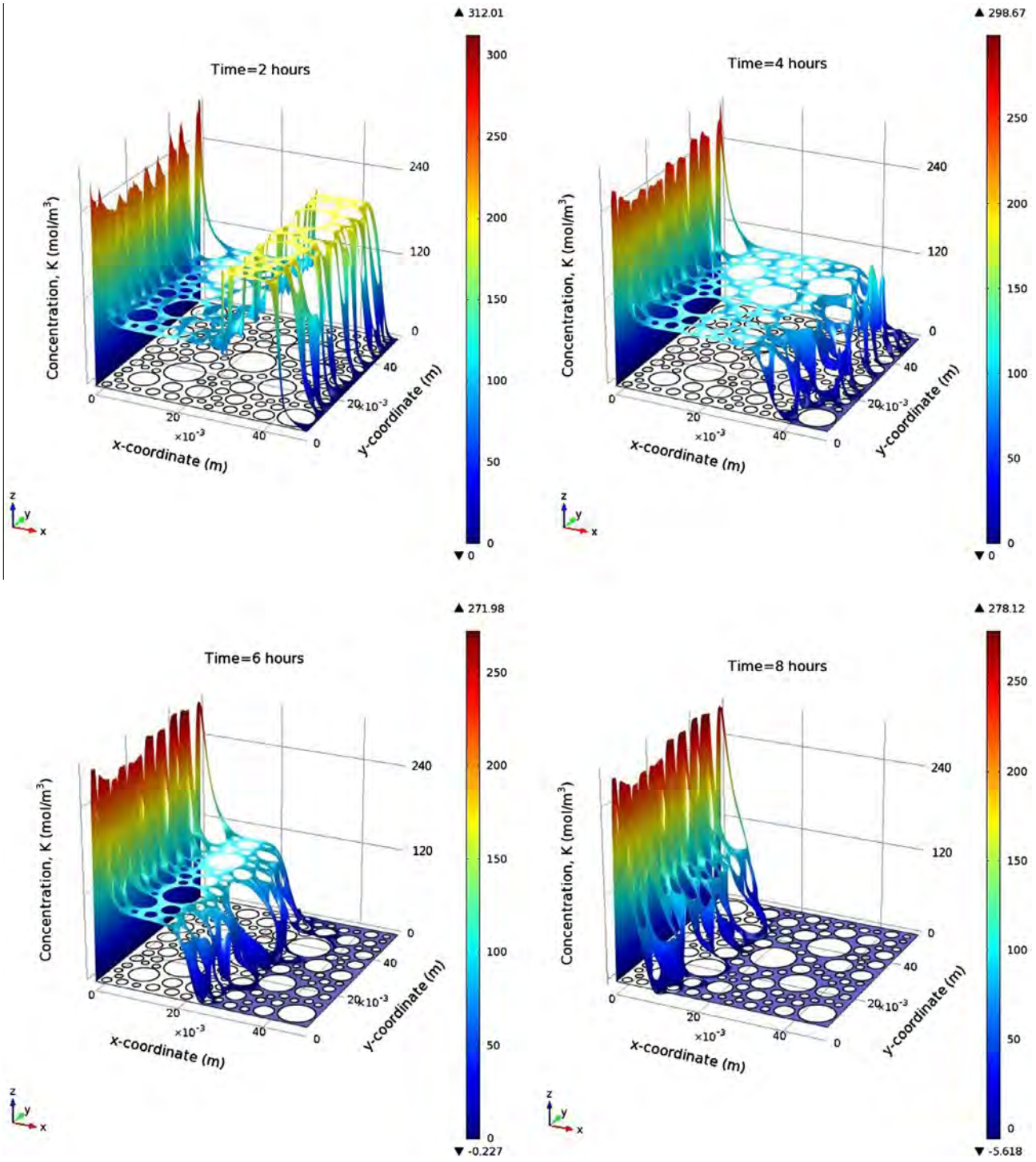

Fig. 5b. Concentration distribution profiles of potassium ions at four different times.

sodium, chloride and hydroxyl. Note that other ionic species (such as calcium and sulphate) may also exist in the concrete. However, owing to their low concentrations they are not considered in the present simulations. Fig. 4 graphically displays the simulation model. Also, since the volume of each compartment is much greater than that of the specimen, it is reasonable to assume that the concentrations of each ionic species in the two compartments remain constant during the migration test. Table 2 shows the initial and boundary conditions employed in the present study.

Experimental results showed that chloride ions can be bounded to solid surfaces while they transport through the pore solution, or vice versa [8]. However, whether the other ionic species have a similar feature remains unknown. In the present study, the chloride binding is used based on the experimental data [8], while the binding of other three species is simply assumed to have an equal binding capacity and is calculated based on the charge balance.

5. Results of FEA simulations

The governing Eqs. (4) and (7) are solved numerically using commercial software COMSOL in the three-phase domain. The five

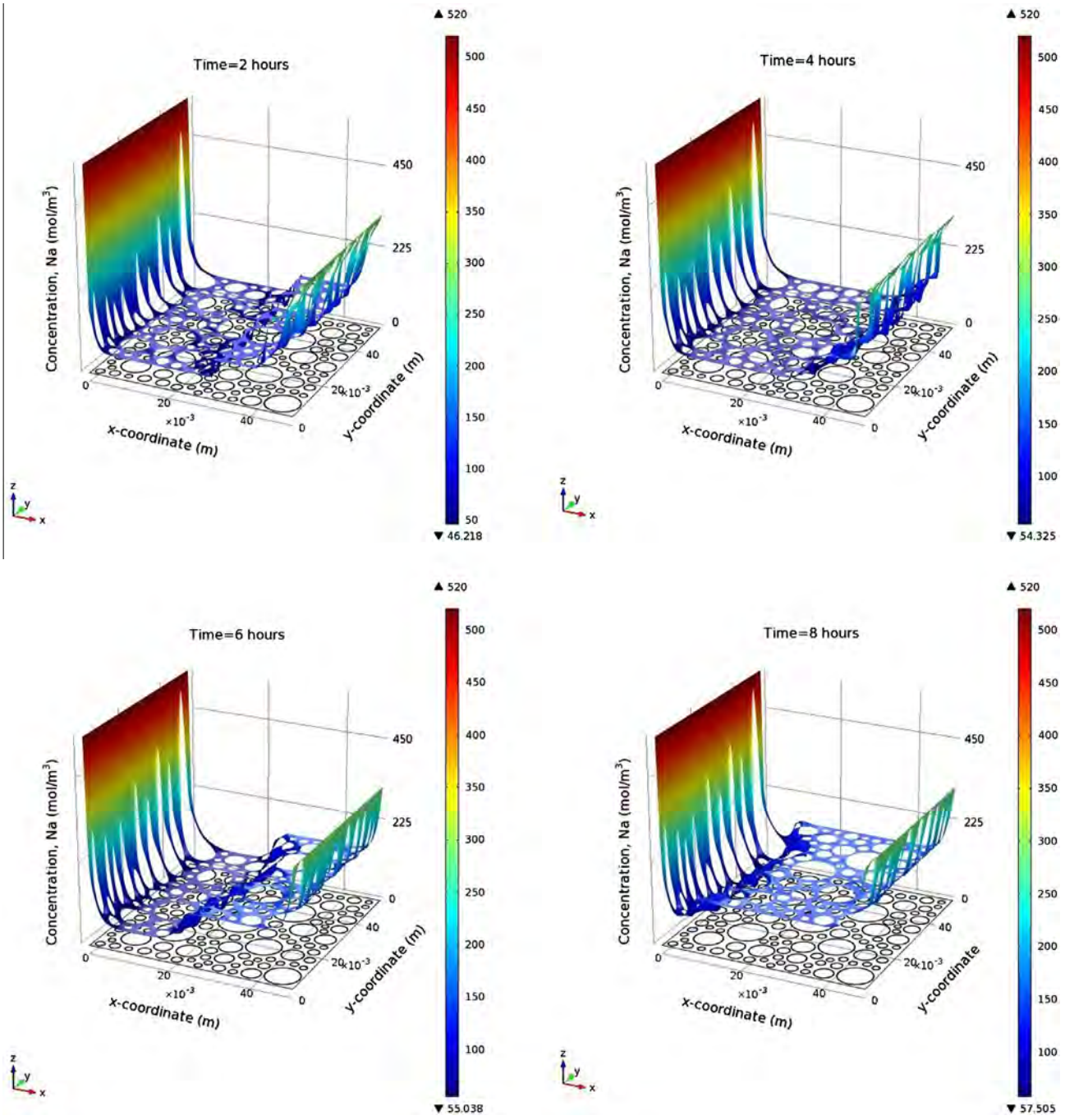

Fig. 5c. Concentration distribution profiles of sodium ions at four different times.

field variables represent the electrostatic potential and four ionic concentrations. Fig. 5 shows the distribution profiles of the five field variables at four different times for the plain concrete with 50% volume fraction of aggregates, in which the two plane coordinates represent the position of the variable in the 2-D concrete model and the vertical coordinate is the value of the variable. Each frame of individual variable represents one instantaneous moment during the RCM test. The 3-D plots provide a good overall view on the evolution of transport of four ionic species in the specimen. The overall patterns of the 3-D plots shown in Fig. 5 are found to be similar to those provided in the 2-phase, multi-component model without taking into account ionic binding [38], but there are some clear distinctive features. These are reflected by the significant different travel speeds between positive and negative charged ions, the concentrations of ionic species at the wave front, and the large difference of gradients of electrostatic potential in the regions near anode and cathode, indicating the influences of ITZs and ionic binding on the transport of ions in concrete. Note that the concentration profiles of the two positively charged species (potassium and sodium) are plotted at 2, 4, 6, and 8 h whereas those of the two negatively charged species (chloride and hydroxyl) are plotted at 1, 2, 3, and 4 h. This is because the travel speed of the positive charged ions is very slow in the first few hours. This again highlights the effect of ionic binding and ITZs on ionic transport.

To quantitatively examine the influence of ITZs and ionic binding on the transport of chloride ions in concrete, the 3-D plots of

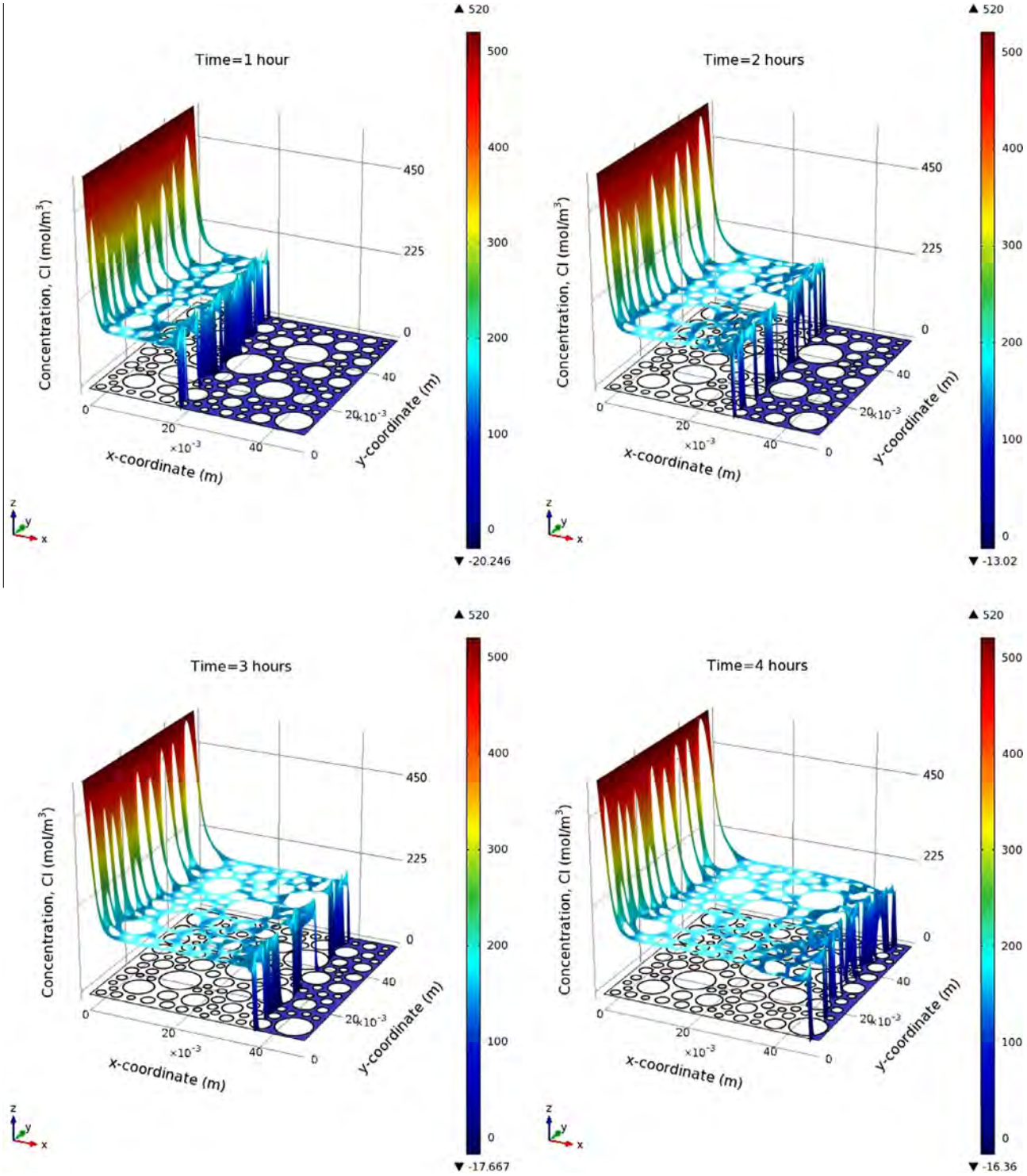

Fig. 5d. Concentration distribution profiles of chloride ions at four different times.

chloride concentration profiles are represented using traditional 2-D plots with concentration against travel distance, as shown in Fig. 6, in which the concentration is the average concentration along the *y*-axis. Since the focus of discussion is on chloride ions only, the 2-D profiles of other ionic species are not re-plotted further here. Obviously, the chloride distribution profile obtained from the presented multi-component model is totally different with those from the previous single-component (i.e. only the chlorides) results [9,47]. This evidently demonstrates the significant influence on the chloride migration caused by multi-species coupling.

For the purpose of investigating the ITZ and binding effects, the results without ITZs (i.e., assuming the same diffusion coefficients in ITZs as those in cement paste) and that without ionic binding are also shown in Figs. 7 and 8, respectively. It is apparent from the comparisons of these three figures that, the ITZs and the ionic binding have adverse influences on the chloride transport. Ignoring ITZs in the model, chloride transport will be under-predicted, not

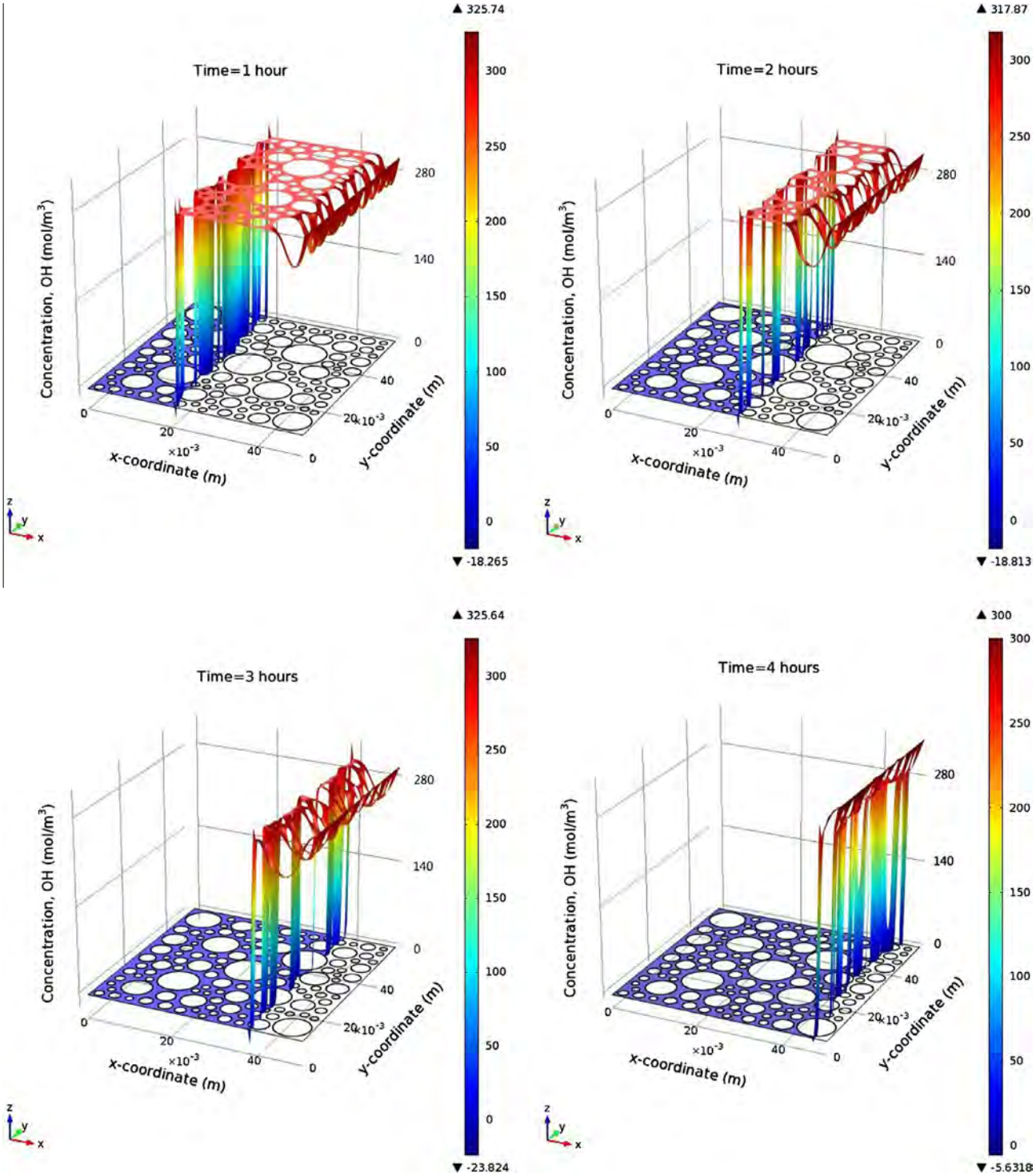

Fig. 5e. Concentration distribution profiles of hydroxide ions at four different times.

only the speed but also the concentration at the wave front. However, if the ITZs are taken into account but the ionic binding is ignored in the model, the chloride transport will be over-predicted, including both the speed and concentration at the wave front. For example, the penetration depth and corresponding concentration of chlorides at 1 h are 0.013 m and 130 mol/m^3 in the model ignoring ITZs (i.e. 2-phase model with ionic binding); while they are 0.019 m and 214 mol/m^3 in the 3-phase model ignoring ionic binding, and 0.017 m and 150 mol/m^3 in the 3-phase model with ionic binding. It is interestingly observed from the 2-D plots shown in Figs. 6–8 that the wave fronts are not the "steep" lines but exhibit gradual decrease with the distance. This feature is not seen from the single phase model [21]. A careful examination of the section plots at different y-values from 3-D results shows that all wave fronts exhibit more or less steep. However, the section profiles are not allied at the same depth at the same time due to the effect

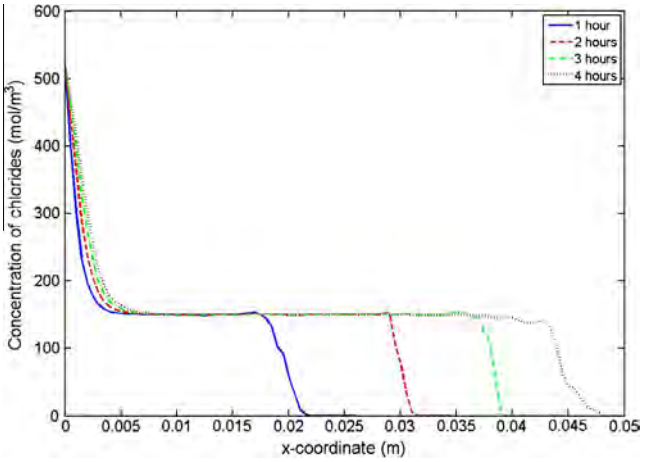

Fig. 6. 2-D plot of concentration distribution profiles of chloride ions in 3-phase model with ionic binding.

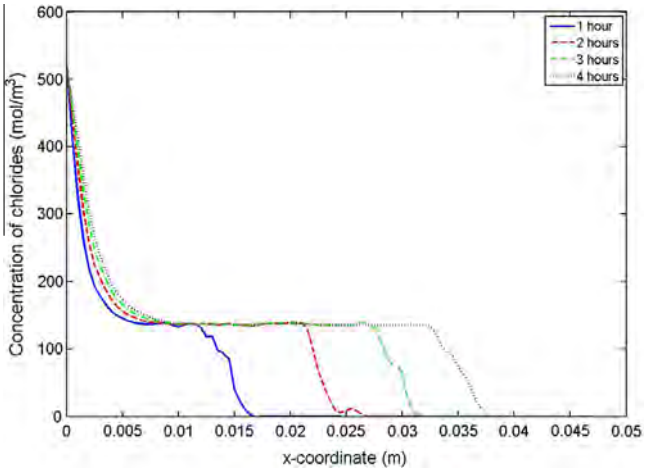

Fig. 7. 2-D plot of concentration distribution profiles of chloride ions in 2-phase model with ionic binding.

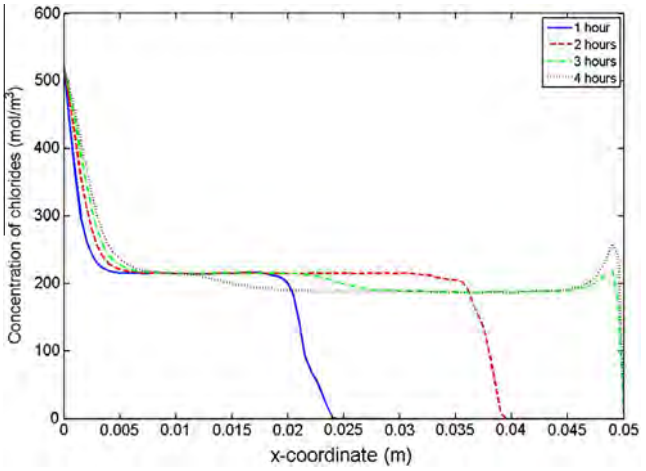

Fig. 8. 2-D plot of concentration distribution profiles of chloride ions in 3-phase model without ionic binding.

of aggregates and ITZs. This leads the concentration at a wave front to decrease with the depth.

6. Chloride diffusion coefficient in concrete

There are two methods which can be used to calculate the chloride diffusion coefficient. One is the steady state migration test [53], in which the chloride diffusion coefficient is calculated as follows,

$$D_{con} = \frac{RTL}{FU} \times \frac{J_2}{C_1} \tag{9}$$

where D_{con} is the overall diffusion coefficient of chlorides in the specimen, L is the specimen length, U is the applied voltage, J_2 is the flux of chlorides at downstream boundary, C_1 is the concentration of chlorides at upstream boundary. Note that Eq. (9) is obtained from the solution of the Fick's second law of the transport of a single species. It is obvious from the concentration distribution profiles shown in Figs. 6–8 that the chloride concentration at the wave front is much lower than that at the upstream boundary. Thus, the chloride diffusion coefficient obtained using Eq. (9) may not be very accurate. Additionally, note that Eq. (9) is valid only when the applied electrical field is high and a full equation valid whatever the voltage value was proposed by Amiri et al. [54]. The other is the non-steady state migration test (also called as RCM test) [9], in which the chloride diffusion coefficient is calculated as follows,

$$D_{con} = \frac{RTL}{FU} \times \frac{x_d - 2\sqrt{\frac{RTLx_d}{FU}}\,\mathrm{erf}^{-1}\left(1 - \frac{2C_d}{C_1}\right)}{t_d} \tag{10}$$

where x_d is the penetration depth of chloride ions at a test duration t_d, C_d is the chloride concentration at the depth x_d, and erf^{-1} is the inverse version of error function. The RCM test method was first proposed by Tang and Nilsson [9], and then adopted as NT Build 492 [55] and AASHTO provisional Standard TP64 [56]. The test is very similar with the rapid chloride permeability test. However, it allows direct measurement by the depth of chloride penetration instead of using the total passed charge to estimate the permeability. RCM has been widely used to measure the diffusion coefficient of chloride ions in concrete. Several RCM tests have shown that Eq. (10) is more reliable than Eq. (9) [57]. Hence, it is also used here to compare the results obtained from different models. Note that neither Eq. (9) nor Eq. (10) takes into account the chloride binding. Also, Eq. (10) is derived from the transport of a single ionic species in a single phase medium. Nevertheless, if one knows the chloride concentration, penetration depth and corresponding penetration time from a multi-component, multiphase model, the overall chloride diffusion coefficient of the concrete can be calculated using Eq. (10).

In RCM tests, the specimen is normally 50 mm thick in which the sizes of aggregates are very restrained in order to provide a good representation of the tested material [55,56]. Therefore the volume fraction of aggregates in the tested specimen is largely limited due to the workability [32]. Furthermore, the largest volume fraction of aggregates employed in existing numerical simulations for chloride transport is about 0.6 or less [38,43,44,47]. This is probably due to the availability of experimental data. For this reason, a set of simulations with different volume fractions of aggregates ranging from 0 to 0.6 are performed in this study. The calculated normalized chloride diffusion coefficient, D_{con}/D_0, where D_0 is the chloride diffusion coefficient used in the cement paste phase, are listed in Table 3 and plotted in Fig. 9. To validate the results obtained from the numerical model, an accelerated chloride migration test brought by Yang and Su [32] is employed as a reference. The experiment consists of mortars made with ASTM Type I

Table 3
Normalized diffusion coefficients (3-phase model with binding effect).

Aggregate volume fraction, V_a	0%	10%	20%	30%	40%	50%	60%
t_d (s)	3600	3600	3600	3600	3600	3600	3600
x_d (m)	0.0250	0.0219	0.0203	0.0192	0.0182	0.0173	0.0159
C_d (mol/m^3)	214.4	146.0	146.0	146.0	146.0	146.0	146.0
D_{con} (10^{-10} m^2/s)	3.6624	3.1234	2.8904	2.7304	2.5850	2.4543	2.2510
D_{con}/D_0	1.0000	0.8528	0.7892	0.7455	0.7058	0.6701	0.6146

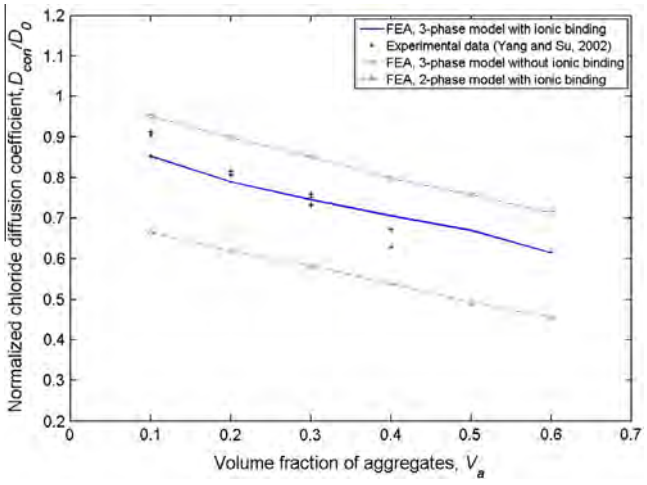

Fig. 9. Comparisons of chloride diffusion coefficients in concrete obtained from different FEA models and experimental data.

Table 4
Normalized diffusion coefficients (3-phase model without binding effect).

Aggregate volume fraction, V_a	0%	10%	20%	30%	40%	50%	60%
t_d (s)	3600	3600	3600	3600	3600	3600	3600
x_d (m)	0.0250	0.0238	0.0225	0.0213	0.0200	0.0190	0.179
C_d (mol/m^3)	214.4	214.4	214.4	214.4	214.4	214.4	214.4
D_{con} (10^{-10} m^2/s)	3.6624	3.4854	3.2936	3.1166	2.9249	2.7774	2.6153
D_{con}/D_0	1.0000	0.9517	0.8993	0.8510	0.7986	0.7584	0.7141

Table 5
Normalized diffusion coefficients (2-phase model with binding effect).

Aggregate volume fraction, V_a	0%	10%	20%	30%	40%	50%	60%
t_d (s)	3600	3600	3600	3600	3600	3600	3600
x_d (m)	0.0250	0.0172	0.0160	0.0151	0.0140	0.0128	0.119
C_d (mol/m^3)	214.4	146.0	146.0	146.0	146.0	146.0	146.0
D_{con} (10^{-10} m^2/s)	3.6624	2.4397	2.2655	2.1349	1.9755	1.8017	1.6716
D_{con}/D_0	1.0000	0.6662	0.6186	0.5829	0.5394	0.4920	0.4564

Portland cement and fine aggregates selected at 0%, 10%, 20%, 30% and 40% volume fractions. 50 mm thick samples were cast and cured in water (23 °C) for 12 months. The experiment results of the normalized diffusion coefficient (D_{con}/D_0) are superimposed in Fig. 9. For examining the influences of ITZs and ionic binding, the results of D_{con}/D_0 obtained from the models without considering ITZs and those without ionic binding (see Tables 4 and 5) are also superimposed in the figure. Note that, owing to the existence of diffusion layer near cathode and the variation of chloride concentration on the wave front, which point on the wave front should be taken for x_d and C_d to calculate the diffusion coefficient in Eq. (10) is crucial. After calibration using experimental data [32] it is found the best point for (x_d, C_d) is the one at the first crest point of the wave front. This point represents the overall migration of chlorides in the 3-phase model.

It is evident from Fig. 9 that the model with both ITZs and ionic binding being taken into account agrees well with the experiment data [32], particularly for the volume fractions equal or less than 0.3. The maximum deviation from the average value of experimental data is only 7.25% for the aggregate volume fraction at 0.4. In contrast, when the ITZ phase or the ionic binding is ignored, the predicted diffusion coefficient is far off from the experimental data. It may be noticed from the figure that there is a slight difference in the slope between the simulations and experiments. This could be due to the over use of the ITZs volume in the simulation when the volume fraction of aggregates is large; while in the reality the volume of ITZs may not be linearly proportional to the volume of aggregates.

7. Conclusions

This paper has presented a 2-D, 3-phase, multi-component ionic transport model for describing the penetration of chlorides in concrete. The model also considers the binding of ions in the solid phase of concrete. The present model has been applied to simulate the RCM test to predict the chloride diffusion coefficient in concrete. From the results obtained the following conclusions can be drawn.

(1) The multi-species coupling has important influence on the electrostatic potential predicted in the multi-phase model. It significantly affects the migration speeds of ionic species. The influences on ionic species with different charges are considerably different.
(2) The inclusion of ITZs in the multi-phase transport model can provide more accurate simulation results. ITZs can accelerate the ionic transport, resulting in a larger transport rate and significantly deeper penetration front. This is mainly due to the use of larger diffusion coefficients of ions in the ITZs. In contrast, ionic binding is equally important in the multi-phase transport model. It can slow down the transport rate of ions in concrete. The influence of ionic binding on ionic transport is opposite to that of ITZs, and also slightly less than that of ITZs.
(3) The present multi-phase model can be used to evaluate the overall diffusion coefficient of chlorides in concrete employed in other simple prediction models, which is demonstrated by available experimental results.

Acknowledgements

The work was supported by the European Research Council via a research grant (FP7-PEOPLE-2011-IRSES-294955). The third author would also like to thank the funding from Shanghai Pujiang Program, P.R. China (13PJ1405200) and State Key Laboratory of Ocean Engineering Youth Innovation Fund (GKZD010059-26).

References

[1] Aitcin PC, Mehta PK. Effect of coarse aggregate characteristics on mechanical properties of high-strength concrete. ACI Mater J 1990;87(2):103–7.
[2] Garboczi EJ. Permeability, diffusivity and microstructural parameters: a critical review. Cem Concr Res 1990;20:591–601.
[3] Escadeillas G, Maso JC. In advances in cementitious materials. 2nd ed. Mindess; 1991.
[4] Diamond S, Huang JD. The ITZ in concrete – a different view based on image analysis and SEM observations. Cem Concr Compos 2001;23(2–3):179–88.
[5] Gao JM, Qian CX, Liu HF, Wang B, Li L. ITZ microstructure of concrete containing GGBS. Cem Concr Res 2005;35(7):1299–304.
[6] Page CL, Short NR, El-Tarras A. Diffusion of chloride ions in hardened cement pastes. Cem Concr Res 1981;11(3):395–406.
[7] Atkinson A, Nickerson AK. The diffusion of ions through water-saturated cement. J Mater Sci 1984;19:3068–78.
[8] Sergi G, Yu SW, Page CL. Diffusion of chloride and hydroxyl ions in cementitious materials exposed to a saline environment. Mag Concr Res 1992;44:63–9.
[9] Tang L, Nilsson LO. Rapid determination of the chloride diffusivity in concrete by applying an electric field. ACI Mater J 1993;89(1):49–53.
[10] Dhir RK, Jones MR, Ng SLD. Prediction of total chloride content profile and concentration/time-dependent diffusion coefficients for concrete. Mag Concr Res 1998;50(1):37–48.
[11] Maheswaran T, Sanjayan JG. A semi-closed-form solution for chloride diffusion in concrete with time-varying parameters. Mag Concr Res 2004;56(6):59–366.
[12] Li LY, Page CL. Modelling of electrochemical chloride extraction from concrete by using electrochemical method. Comput Mater Sci 1998;9:303–8.
[13] Li LY, Page CL. Finite element modelling of chloride removal from concrete by an electrochemical method. Corros Sci 2000;42(12):2145–65.
[14] Truc O, Ollivier JP, Nilsson LO. Numerical simulation of multi-species transport through saturated concrete during a migration test – MSDIFF code. Cem Concr Res 2000;30(10):1581–92.
[15] Truc O, Ollivier JP, Nilsson LO. Numerical simulation of multi-species diffusion. Mater Struct 2000;33(233):566–73.
[16] Wang Y, Li LY, Page CL. A two-dimensional model of electrochemical chloride removal from concrete. Comput Mater Sci 2001;20(2):196–212.
[17] Krabbenhoft K, Krabbenhoft J. Application of the Poisson–Nernst–Planck equations to the migration test. Cem Concr Res 2008;38(1):77–88.
[18] Friedmann H, Amiri O, Ait-Mokhtar A. Shortcomings of geometrical approach in multi-species modelling of chloride migration in cement-based materials. Mag Concr Res 2008;60(2):119–24.
[19] Elakneswaran Y, Iwasa A, Nawa T, Sato T, Kurumisawa K. Ion-cement hydrate interactions govern multi-ionic transport model for cementitious materials. Cem Concr Res 2010;40(12):1756–65.
[20] Johannesson B, Yamada K, Nilsson LO, Hosokawa Y. Multi-species ionic diffusion in concrete with account to interaction between ions in the pore solution and the cement hydrates. Mater Struct 2007;40(7):651–65.
[21] Xia J, Li LY. Numerical simulation of ionic transport in cement paste under the action of externally applied electric field. Constr Build Mater 2013;39:51–9.
[22] Bentz DP, Garboczi EJ. Percolation of phases in a three-dimensional cement paste microstructural model. Cem Concr Res 1991;21(2–3):325–44.
[23] Bourdette B, Ringot E, Ollivier JP. Modeling of the transition zone porosity. Cem Concr Res 1995;25(4):741–51.
[24] Garboczi EJ, Schwartz LM, Bentz DP. Modelling the influence of the interfacial zone on the conductivity and diffusivity of concrete. J Adv Cem-Based Mater 1995;2:169–81.
[25] Delagrave A, Bigas JP, Ollivier JP, Marchand J, Pigeon M. Influence of the interfacial zone on the chloride diffusivity of mortars. Adv Cem Based Mater 1997;5(3–4):86–92.
[26] Garboczi EJ, Bentz DP. Analytical formulas for interfacial transition zone properties. Adv Cem Based Mater 1997;6(3–4):99–108.
[27] Garboczi EJ, Bentz DP. Multiscale analytical/numerical theory of the diffusivity of concrete. Adv Cem Based Mater 1998;8(2):77–88.
[28] Hobbs DW. Aggregate influence on chloride ion diffusion into concrete. Cem Concr Res 1999;29:1995–8.
[29] Xi Y, Bazant ZP. Modeling chloride penetration in saturated concrete. J Mater Civ Eng 1999:58–65.
[30] Bentz DP, Jensen OM, Coats AM. Influence of silica fume on diffusivity in cement-based materials, I. experimental and computer modeling studies on cement pastes. Cem Concr Res 2000;30(6):953–62.
[31] Shane JD, Mason TO, Jennings HM. Effect of the interfacial transition zone on the conductivity of Portland cement mortars. Am Ceram Soc 2000;83(5):1137–44.
[32] Yang CC, Su JK. Approximate migration coefficient of interfacial transition zone and the effect of the aggregate content on the migration coefficient of mortar. Cem Concr Res 2002;32(10):1559–65.
[33] Caré S. Influence of aggregates on chloride diffusion coefficient into mortar. Cem Concr Res 2003;33(7):1021–8.
[34] Caré S, Hervé E. Application of a n-phase model to the diffusion coefficient of chloride in mortar. Transp Porous Media 2004;56(2):119–35.
[35] Byung HO, Seung YJ. Prediction of diffusivity of concrete based on simple analytical equations. Cem Concr Res 2004;34(3):463–80.
[36] Yang CC, Weng SH. A three-phase model for predicting the effective chloride migration coefficient of ITZ in cement-based materials. Mag Concr Res 2013;65(3):193–201.
[37] Ying JW, Xiao JZ, Shen LM, Bradford MA. Five-phase composite sphere model for chloride diffusivity prediction of recycled aggregate concrete. Mag Concr Res 2013;65(9):573–88.
[38] Liu QF, Li LY, Easterbrook D, Yang J. Multi-phase modelling of ionic transport in concrete when subjected to an externally applied electric field. Eng Struct 2012;42:201–13.
[39] Zeng YW. Modeling of chloride diffusion in hetero-structured concretes by finite element method. Cem Concr Compos 2007;29:559–65.
[40] Zheng JJ, Zhou XZ. Prediction of the chloride diffusion coefficient of concrete. Mater Struct 2007;40:693–701.
[41] Zheng JJ, Wong HS, Buenfeld NR. Assessing the influence of ITZ on the steady-state chloride diffusivity of concrete using a numerical model. Cem Concr Res 2009;39:805–13.
[42] Zheng JJ, Zhou XZ, Wu YW, Jin XY. A numerical method for the chloride diffusivity in concrete with aggregate shape effect. Constr Build Mater 2012;31:151–6.
[43] Li LY, Xia J, Lin SS. A multi-phase model for predicting the effective diffusion coefficient of chlorides in concrete. Constr Build Mater 2012;26(1):295–301.
[44] Abyaneh SD, Wong HS, Buenfeld NR. Modelling the diffusivity of mortar and concrete using a three-dimensional mesostructure with several aggregate shapes. Comput Mater Sci 2013;78:63–73.
[45] Friedmann H, Amiri O, Aït-Mokhtar A. Physical modelling of the electrical double layer effects on multispecies ions transport in cement-based materials. Cem Concr Res 2008;38(12):1394–400.
[46] Nguyen PT, Amiri O. Study of electrical double layer effect on chloride transport in unsaturated concrete. Constr Build Mater 2014;50:492–8.
[47] Šavija B, Luković M, Schlangen E. Lattice modeling of rapid chloride migration in concrete. Cem Concr Res 2014;61–62:49–63.
[48] Liu Y, Shi X. Ionic transport in cementitious materials under an externally applied electric field: finite element modeling. Constr Build Mater 2012;27:450–60.
[49] Liu QF, Xia J, Easterbrook D, Yang J, Li LY. Three-phase modeling of electrochemical chloride removal from corroded steel-reinforced concrete. Constr Build Mater 2014;70:410–27.
[50] Liu QF. Multi-phase modelling of multi-species ionic migration in concrete. PhD thesis, University of Plymouth; 2014.
[51] Li LY. A pore size distribution-based chloride transport model in concrete. Mag Concr Res 2014;66(18):937–48.
[52] Jiang JY, Sun GW, Wang CH. Numerical calculation on the porosity distribution and diffusion coefficient of interfacial transition zone in cement-based composite materials. Constr Build Mater 2013;39:134–8.
[53] NT-Build 335. Concrete, mortar and cement-based repair materials: chloride diffusion coefficient from migration cell experiments. Nordtest, Esbo, Finland; 1997.
[54] Amiri O, Aït-Mokhtar A, Seigneurin A. A complement to the discussion of Xu A., Chandra S., calculation of chloride diffusion coefficients in concrete from ionic migration measurements by Andrade C. Cem Concr Res 1997;27(6):951–7.
[55] NT-Build 492. Nordtest method: concrete, mortar and cement-based repair materials: chloride migration coefficient from non-steady-state migration experiments; 1999.
[56] AASHTO TP 64-03. Standard method of test for prediction of chloride penetration in hydraulic cement concrete by the rapid migration procedure. American Association of State Highway and Transportation Officials, Washington; 2003.
[57] Tang L. Electrically accelerated methods for determining chloride diffusivity in concrete – current development. Mag Concr Res 1996;48(176):173–9.